Oncogene (2011) 30, 2319–2332

www.nature.com/onc

ORIGINAL ARTICLE

Essential role of microphthalmia transcription factor for DNA replication, mitosis and genomic stability in melanoma

T Strub[1,4], S Giuliano[2,4], T Ye[1], C Bonet[2], C Keime[1], D Kobi[1], S Le Gras[1], M Cormont[3], R Ballotti[2], C Bertolotto[2] and I Davidson[1]

[1]*Institut de Génétique et de Biologie Moléculaire et Cellulaire, CNRS, INSERM, Université de Strasbourg, Illkirch, France;* [2]*INSERM U895 Team 1 and Department of Dermatology, CHU Nice, France and* [3]*INSERM U895 Team 7, Nice, France*

Malignant melanoma is an aggressive cancer known for its notorious resistance to most current therapies. The basic helix-loop-helix microphthalmia transcription factor (MITF) is the master regulator determining the identity and properties of the melanocyte lineage, and is regarded as a lineage-specific 'oncogene' that has a critical role in the pathogenesis of melanoma. MITF promotes melanoma cell proliferation, whereas sustained supression of MITF expression leads to senescence. By combining chromatin immunoprecipitation coupled to high throughput sequencing (ChIP-seq) and RNA sequencing analyses, we show that MITF directly regulates a set of genes required for DNA replication, repair and mitosis. Our results reveal how loss of MITF regulates mitotic fidelity, and through defective replication and repair induces DNA damage, ultimately ending in cellular senescence. These findings reveal a lineage-specific control of DNA replication and mitosis by MITF, providing new avenues for therapeutic intervention in melanoma. The identification of MITF-binding sites and gene-regulatory networks establish a framework for understanding oncogenic basic helix-loop-helix factors such as N-myc or TFE3 in other cancers.
Oncogene (2011) **30,** 2319–2332; doi:10.1038/onc.2010.612; published online 24 January 2011

Keywords: senescence; DNA repair; cancer; metastasis

Introduction

Micropthalmia transcription factor (MITF) is a basic helix-loop-helix protein that is the master regulator determining the identity and properties of the melanocyte lineage (Goding, 2000a, b). The *MITF* locus encodes multiple isoforms from alternate splicing and use of internal promoters (Steingrimsson, 2008). The MITF-M isoform (hereafter designated simply as MITF) is the major form produced specifically in the melanocyte lineage from an intronic promoter (Goding, 2000b). MITF is essential for the survival of melanoblasts and postnatal melanocytes (McGill *et al*., 2002; Hou and Pavan, 2008), in which it also controls the expression of genes required for the melanin synthesis (Bertolotto *et al*., 1998).

In addition to regulating multiple aspects of normal melanocyte function, MITF also has a critical role in melanoma, in which it is required for survival, and controls the proliferation, invasive and metastatic properties of melanoma cells (Garraway *et al*., 2005a, b; Goodall *et al*., 2008; Pinner *et al*., 2009). Primary and metastatic melanoma lesions comprise populations of cells expressing high and low MITF levels. Cells expressing low levels of MITF show high levels of the POU3F2 (BRN2) transcription factor that binds to the MITF promoter and represses its transcription (Goodall *et al*., 2008; Kobi *et al*. 2010). These cells show reduced proliferation, but enhanced motility and invasiveness, whereas higher levels of MITF are associated with enhanced proliferative capacity. Melanoma cells seem to switch between these two states during tumour progression (Hoek *et al*., 2008a). Recently, it has also been shown that sustained MITF suppression triggers senescence of melanoma cells (Giuliano *et al*. 2010). Hence, depending on its expression level, MITF can have pro- or anti-proliferative effects.

To better understand the function of MITF in melanoma and to more generally define the molecular basis of its function in the melanocyte lineage, we have performed chromatin immunoprecipitation coupled to high throughput sequencing (ChIP-seq) experiments in human 501Mel cells and RNA sequencing (RNA-seq) following small interfering RNA (siRNA)-mediated MITF knockdown. Our results show direct MITF regulation of an extensive set of genes required for DNA replication, repair and mitosis. This lineage-specific control of replication and mitosis explains how MITF promotes melanoma proliferation, and suggests a mechanism by which diminished MITF expression in melanoma lesions may favour genomic instability and the emergence of more aggressive metastatic cells.

Correspondence: C Bertolotto, INSERM U895 Team 1 and Department of Dermatology, CHU Nice, France.
E-mail: corine.bertolotto@unice.fr or I Davidson, CNRS; INSERM; Université de Strasbourg, IGBMC, 1 Rue Laurent Fries, Illkirch Cédex 67404, France.
E-mail: irwin@igbmc.fr
[4]These authors contributed equally to this work.
Received 22 September 2010; revised 20 October 2010; accepted 20 October 2010; published online 24 January 2011

Results

Identification of MITF-binding sites in human 501Mel cells

Human 501Mel cells are considered as having a high proliferative, low invasive phenotype *in vitro*, are poorly tumourigenic when injected subcutaneously in nude mice and express high levels of MITF (Moore *et al*., 2004; Goodall *et al*., 2008; and see Supplementary Figure 1A, lane 1). To facilitate ChIP-seq in these cells, we generated clonal lines expressing 3 × hemagglutinin (HA)-tagged MITF at levels comparable with the endogenous (Supplementary Figure 1A). Anti-HA ChIP–quantitative PCR (qPCR) showed MITF occupancy of three previously identified binding sites in the promoters of the tyrosinase (*TYR*; Bentley *et al*., 1994), hypoxia inducible factor 1a (*HIF1A*; Busca *et al*., 2005) and *RAB27A* (Chiaverini *et al*., 2008) genes, but not at the protamine 1 (*PRM1*) promoter used as a negative control (Supplementary Figure 1B). Although the anti-HA ChIP showed strong enrichment only in the cells expressing the tagged MITF, polymerase II (Pol II) was observed at the *TYR*, *HIF1A* and *RAB27A*, but not the *PRM1* promoters in both the tagged and native 501Mel cells (Supplementary Figure 1C).

Having demonstrated the specificity of the anti-HA ChIP, we then performed anti-HA ChIP-seq on the tagged and native 501Mel cells along with ChIP against Pol II and mono- and tri-methylated lysine 4 of histone H3. After peak detection and annotation (Experimental procedures in Supplementary Information), 1 2139 MITF-occupied loci were identified (see Supplementary Table 1 showing the genomic localisation of the MITF occupied sites and their nearby transcripts). Of these, 9447 sites were located within ± 20 kb of annotated RefSeq genes, 43% of which were located within −5/ + 10 kb of annotated transcription start sites (Figure 1a). Promoter proximal MITF-binding sites are not randomly located within the −5 to + 2kb region, but are preferentially located around 150 bp upstream of the transcription start site, a region that is often nucleosome free in active promoters (Figure 1b). Amongst 1000 highly occupied loci, 822 comprised one or several E-boxes of the type 5′-CACGTG-3′ or 5′-CATGTG-3′, showing that these are preferred sequences, but only four examples of the 'M-box' (5′-AGTCATGTGCT-3′; Bertolotto *et al*., 1998) were observed (see Supplementary Table 2 showing the locations of the E-box sequences at these loci).

A global analysis of the ChIP-seq data using read density matrix clustering based on the coordinates of 1 2139 MITF-occupied loci indicated that around 20% of the MITF-occupied sites were located at promoters with high Pol II and H3K4me3 (Figure 1c). The remaining sites were located either at repressed promoters or distant intergenic regulatory regions. As expected, there was a high convergence of Pol II and H3K4me3 that were both present at essentially the same set of transcription start sites. MITF occupancy seen in ChIP-seq could be confirmed by ChIP–qPCR at a set of known and novel target loci (Figure 1d and see below).

MITF occupies sites at 5578 potential target genes, of which 2771 genes have occupied sites in the proximal promoter (−5/ + 2kb) and 1743 genes in the immediate upstream region (−1000/ + 100 bp; Supplementary Table 1). We observed MITF occupancy of previously identified target genes involved in pigmentation (*TYR*, *DCT*), apoptosis (*BAX*, *BIRC7*; Dynek *et al*., 2008), cell cycle (cyclin-dependent kinase 4, cyclin-dependent kinase 2; Du *et al*., 2004) and transformation (*MET*; Beuret *et al*., 2007). At some genes, the major MITF-occupied site does not correspond to that previously described. For example, there is little or no occupancy of the previously described proximal promoter sites in the *BCL2* and *DIAPH1* genes (McGill *et al*., 2002; Carreira *et al*., 2006), but MITF rather occupies several intronic sites, including major sites towards the 3′ end of the gene (Supplementary Table 1, Supplementary Figure 2B and data not shown). However, we do not see occupancy of the DICER1 promoter that has recently been shown to be a MITF-target gene in melanocytes (Levy *et al*., 2010), suggesting that the repertoire of MITF-occupied genes may differ in melanocytes and melanoma cells. Together these results indicate that MITF occupies a large set of loci and can potentially regulate many target genes.

Identification of MITF-regulated genes in 501MEL cells

To determine which of the potential target genes are regulated by MITF, we used two previously described siRNA sequences to knockdown MITF expression in 501Mel cells (Figure 2a). MITF knockdown resulted in a profound morphological change (Carreira *et al*., 2006) and entry into a senescent state characterised by activation of the DNA damage response, the appearance of senesence-associated heterochromatic foci and β-galactosidase staining (Giuliano *et al*., 2010; and Figure 3). Both the senescence-associated heterochromatic foci and β-galactosidase activity were prominent in the siMITF-knockdown cells that had altered morphology, but not in the control siluciferase (siLUC) cells or in the fraction of siMITF cells that had escaped transfection and did not show the characteristic morphological changes.

To understand how loss of MITF leads to senescence, we performed 3′-end sequencing of RNA from siMITF and control siLUC cells (see Supplementary Table 3 showing the quantitated mRNA expression levels under both conditions and the genes deregulated on MITF knockdown). Comparison of the data sets identified 732 upregulated and 613 downregulated transcripts showing a greater than twofold change (Supplementary Table 3). Upregulated transcripts are primarily associated with ontology terms, such as cytoplasm, signal and cytoskeleton, and cell adhesion and cancer signalling pathways reflecting the changes in cell morphology, and the increased motility and invasiveness of cells with diminished MITF expression (Figures 2b and c and see Supplementary Tables 4 and 5 showing the genes and pathways identified by gene ontology analysis).

In contrast, downregulated transcripts are associated with nucleus, cell cycle, DNA replication and repair and

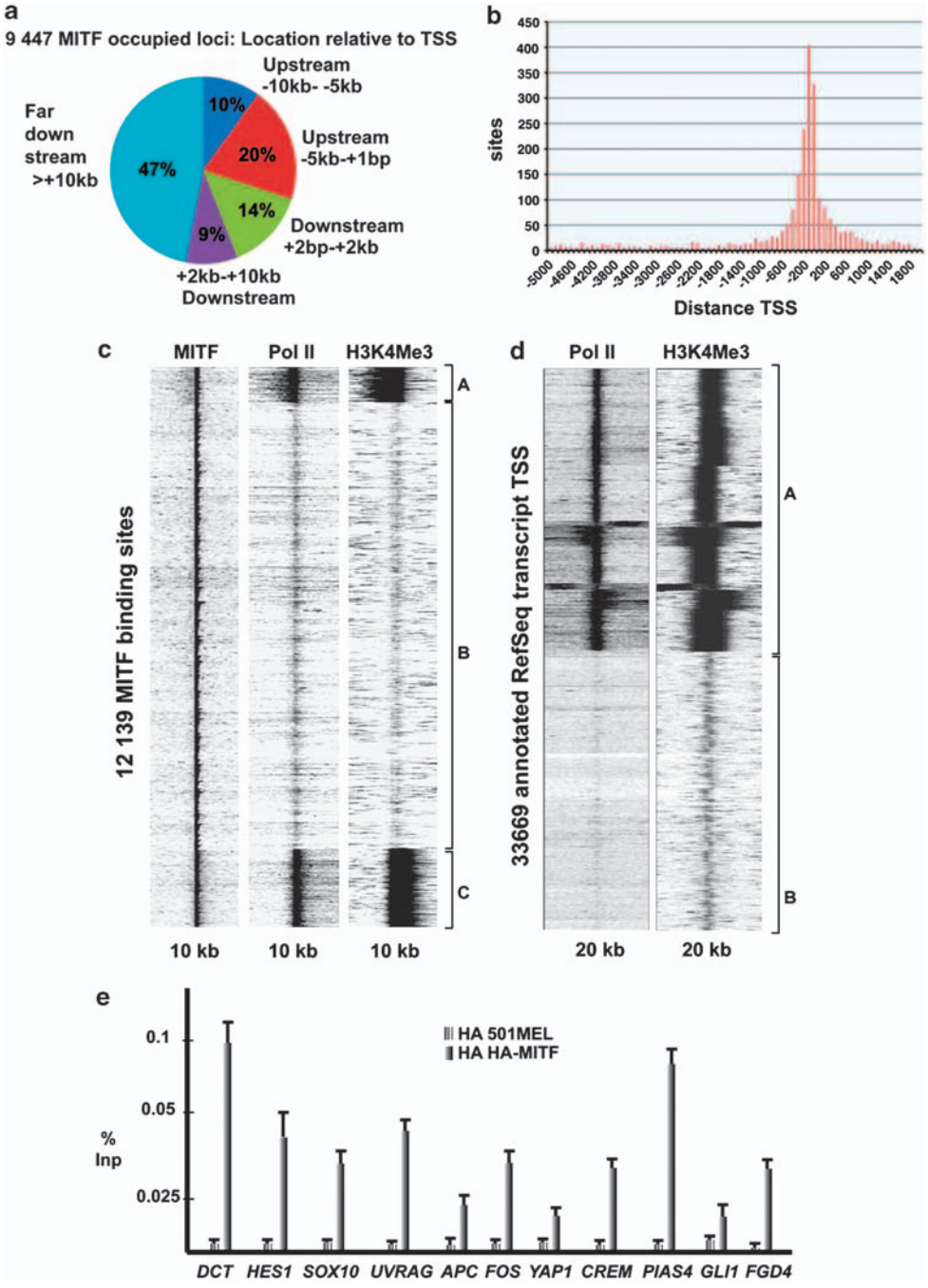

Figure 1 MITF-occupied loci in 501Mel cells. (**a**) A pie chart representation of the location of the MITF-binding sites relative to the transcription start site. (**b**) Preferential location of promoter proximal MITF-occupied sites in proximity to the transcription start site. (**c**) Association of MITF occupancy with Pol II and H3K4me3. Comparison of tag density in the region of ± 5 kb around the MITF-occupied loci. Clustering identifies three major groups: A and C, MITF loci immediately upstream or downstream of promoters with high Pol II and H3K4me3, B: MITF loci with low or no Pol II and H3K4me3 corresponding to repressed promoters or distal regulatory regions. Groups A and C account for around 20% of all MITF-occupied loci. (**d**) Association of Pol II and H3K4me3 at the transcription start site-annotated RefSeq transcripts. Group A, transcription start site with high Pol II and H3K4me3; B, weakly or non-transcribed. (**e**) Anti-HA ChIP–qPCR at MITF-occupied sites identified by ChIP-seq in the promoters of the indicated genes.

mitosis. The up- and downregulated genes, therefore, reflect distinct functional categories. The changes in expression of novel MITF-target genes was also demonstrated by reverse transcriptase–qPCR in independent RNA preparations with in general a good correlation with the RNA-seq data (Figure 2d). Although MITF has previously been considered to be an activator, the observation that many occupied genes are upregulated on MITF knockdown shows that it may function as a repressor at some promoters (see also Supplementary Figure 3).

Comparison of the RNA-seq and ChIP-seq results showed that of the 732 upregulated genes, 225 were

obvious direct targets with associated MITF-occupied sites, whereas 240 downregulated genes were direct targets (Figure 2e and Supplementary Table 3). Hence, only a subset of MITF-bound promoters was deregulated on MITF silencing. Further comparison with data on more than 6000 genes induced on MITF over-

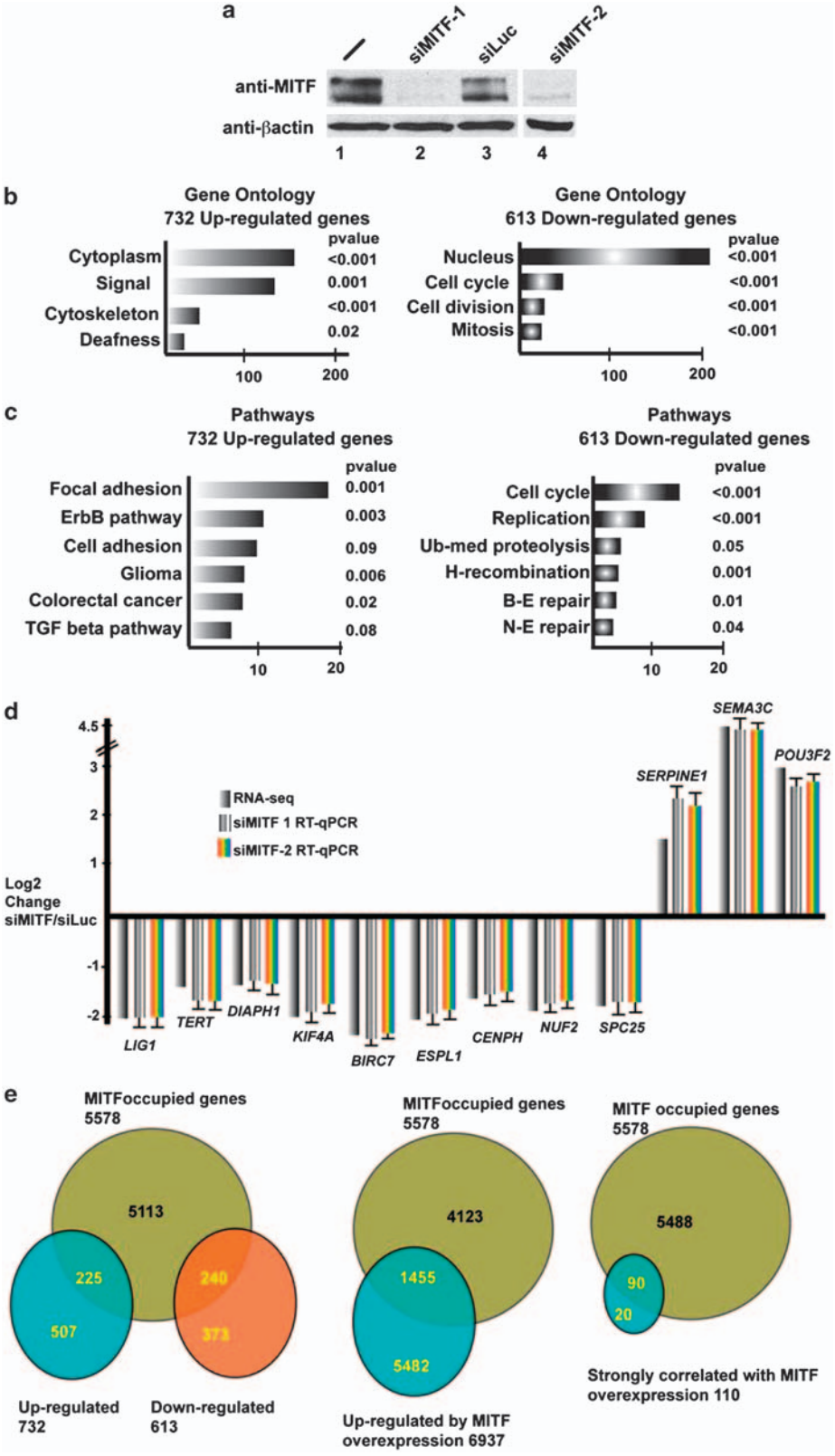

expression by Hoek *et al*., 2008b indicated that 1455 were direct MITF targets (Figure 2e and Supplementary Table 3). Similarly, Hoek *et al*. identified a further 110 genes whose expression correlates closely with that of MITF in melanoma cells of which 90 are direct targets (Figure 2e).

Together these results identify a set of genes that can be directly regulated by loss and/or gain of MITF function in melanoma cells.

MITF regulates genes required for DNA replication

As previously reported, and as shown above, loss of MITF activates the DNA damage response and promotes entry into a senescent state. In accordance with this observation, siMITF silencing resulted in downregulation of at least 31 genes involved in DNA replication, recombination and repair (Figure 4), of which 15 are direct targets of MITF. For example, MITF occupies sites in exon 2 and in downstream introns of the *LIG1* gene (Supplementary Figures 4A and B) encoding DNA ligase 1, involved in the religation of Okazaki fragments during DNA replication, DNA repair and maintenance of genome stability (Tomkinson and Mackey, 1998; Bentley *et al*., 2002). Similarly, genes encoding DNA replication licensing factor MCM2 and the origin recognition complex subunit 6 (*ORC6L*) comprise MITF-occupied sites in their proximal promoters and are repressed on MITF silencing (Figure 4). Furthermore, genes encoding crossover junction endonuclease EME1 (Abraham *et al*., 2003), the replication/repair proteins BRCA1 and FANCA are all closely associated with MITF-occupied sites (Figure 4). These genes encode proteins with well established and interconnected functions in DNA replication, repair and genomic stability (Wang, 2007).

Telomerase reverse transcriptase is required for the proper replication of telomeres and is frequently expressed in human tumours, but not in normal somatic cells (Kim *et al*., 1994; Rudolph *et al*., 1999; Artandi and DePinho, 2000, 2010). RNA-seq and reverse transcriptase–qPCR show that *TERT* is expressed in 501Mel cells and is strongly downregulated on MITF knockdown (Figure 2d). Examination of the *TERT* locus shows H3K4 trimethylation and Pol II occupancy, and reveals a MITF-occupied E-box located in the 5′-untranslated region (Supplementary Figure 4B and C).

To assess the roles of *TERT* and *LIG1* in 501mel cells, we performed siRNA-mediated knockdown (Figure 5a). Loss of either of these proteins led to a significant reduction in cell proliferation (data not shown), but did not induce the same striking morphological changes seen on siMITF (Figure 5b). SiTERT led to the accumulation of distinct populations of slim bipolar or rounded flattened cells, whereas siLIG1 induced the appearance of rounded cells with prominant cytoplasmic prolongations, similar but not identical to siMITF. SiRNA knockdown of *TERT* or *LIG1* also results in activation of the DNA damage response (Figure 5c). Together these observations show that MITF directly regulates the expression of *LIG1*, *TERT* and a collection of replication genes required for normal melanoma cell proliferation.

MITF regulates genes required for normal mitosis

In addition to the genes involved in DNA replication, we further identified a set of 39 genes involved in centromere organization, and mitosis that are downregulated on MITF silencing. Strikingly, MITF occupies sites associated with the *CENPF*, *CENPH* and *CENPM* genes (Figure 4) that are involved in the CENPA–nucleosome associated and CENPA–nucleosome distal complexes (Foltz *et al*., 2006; Carroll *et al*., 2009). Moreover, three of the subunits (*NUF2*, *SPC24* and *SPC25*) of the NDC80 complex that connect kinetochores to the spindle microtubules (Cheeseman *et al*., 2006), as well as *HAUS8*/*HICE1* that interacts with this complex (Wu *et al*., 2008) are all downregulated in siMITF cells. *HAUS8* and *SPC24* are direct targets with neighbouring MITF-occupied sites, as is *CDCA8* encoding the chromosomal passenger complex component Borealin (Figure 4), and TACC3 whose loss leads to defective abscission and binucleate cells (Gomez-Baldo *et al*., 2010). In addition, we also identified MITF-occupied sites in the promoters of genes encoding the G2-specific cyclins B1 and F (*CCNB1*, *CCNF*) that promote entry into mitosis, as well as polo-like kinase 1 (*PLK1*) required for normal melanoma cell mitosis (Schmit *et al*., 2009) and the G1/S cyclin D1 (*CCND1*), a major regulator of cell proliferation. (Figure 4, and Supplementary Figure 5A and B). Expression of the CCNB1, CCND1 and PLK1 proteins was downregulated on siMITF silencing (Supplementary Figure 5C).

The downregulation of the above genes has been shown to induce mitotic defects, suggesting that similar effects should be observed on siMITF silencing (Foltz *et al*., 2006; Ruchaud *et al*., 2007; Carroll *et al*., 2009; Neumann *et al*., 2010). Immunofluorescence after siLUC showed the formation of normal bipolar spindles as illustrated by the staining of the cytoskeletal

Figure 2 Gene expression following siRNA-mediated MITF knockdown. (**a**) Immunoblot of total extracts from cells following transfection of siRNAs against MITF or luciferase as control, β-actin is used as loading control. (**b**, **c**) Gene ontology and Kyoto encyclopedia of genes and genome pathway analysis of the MITF-upregulated and -downregulated transcripts was performed using DAVID (http://david.abcc.ncifcrf.gov/). The number of genes, *P*-value and ontology, or pathway terms for each class are indicated. The full results are provided in Supplementary Tables S4 and S5. Ubiquitin (Ub)-mediated proteolysis, homologous (H) recombination, base excision (B-E) repair and nucleotide excision (N-E) repair. (**d**) Reverse transcriptase–qPCR evaluation of gene expression. The changes in expression of the indicated genes on siMITF knockdown with the two different siRNAs are measured by reverse transcriptase–qPCR and compared with the values obtained by RNA-seq. (**e**) Venn diagrams showing intersection between MITF-occupied genes from ChIP-seq and MITF-regulated genes following siMITF knockdown or overexpression. TGF, transforming growth factor.

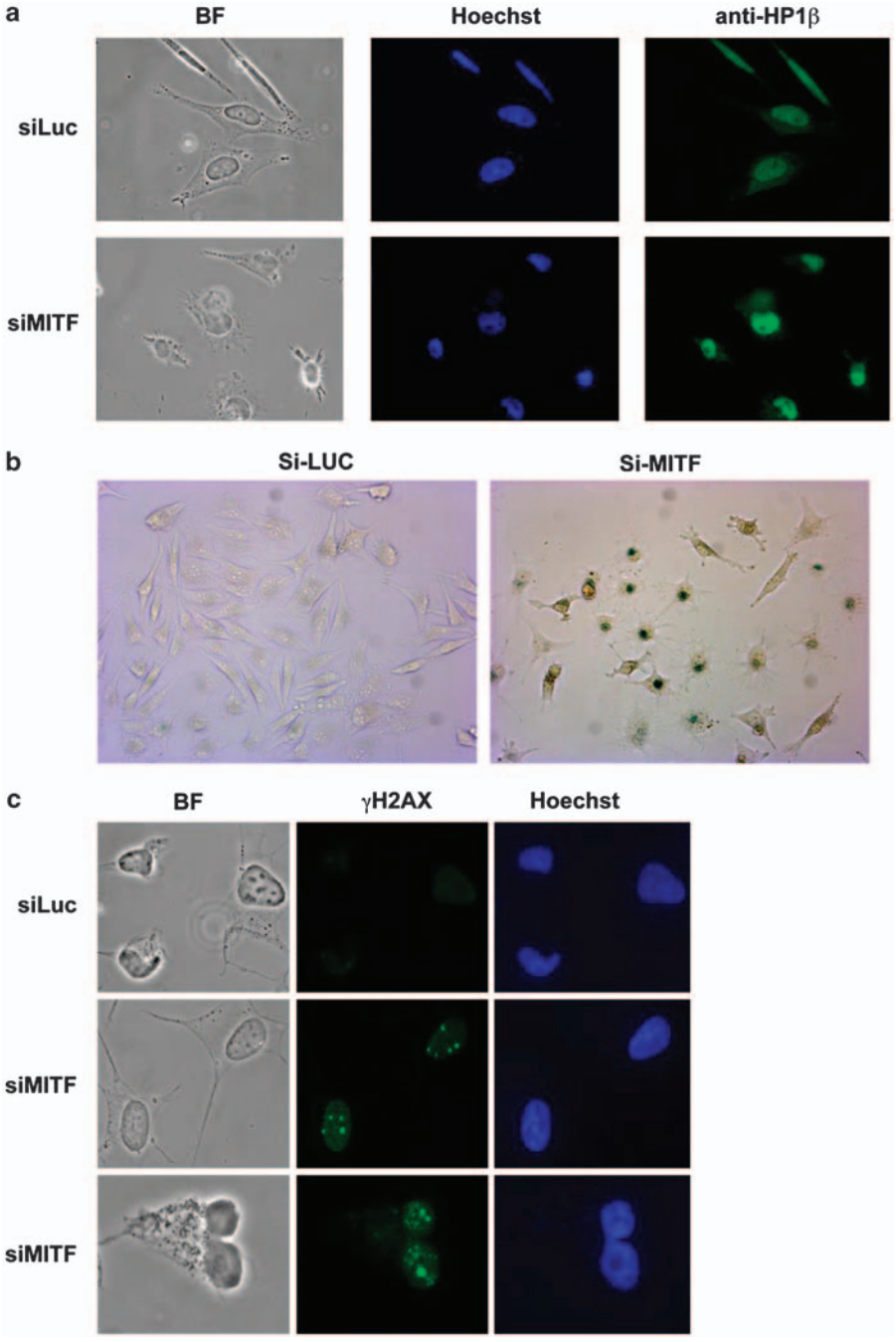

Figure 3 The siRNA-mediated knockdown of MITF leads to senescence and activation of the DNA damage response. (**a**) Immunofluorescence with HP1β antibody to detect senescence-associated heterochromatic foci. Bright field (BF) views, anti-HP1β and Hoechst staining are shown for cells transfected with siMITF or siLUC siRNAs as indicated. (**b**) Cells transfected with the indicated siRNAs were assayed for senescence-associated β-galactosidase activity. (**c**) Cells transfected with the indicated siRNAs were assayed for activation of the DNA damage response using immunofluorescence with antibody against phosphorylated (γ)H2AX. Loss of MITF resulted in the appearance of DNA damage foci that were particularly evident in cells with anaphase bridges due to abnormal mitosis (lower panel). Magnification 10-fold in **b** and 63-fold in **a** and **c**.

microtubule network and mitotic spindle with β-tubulin antibody and highly condensed chromosomes, stained with phosphorylated histone H3Ser10 antibody. During metaphase, chromosomes aligned along the equatorial planes (Figures 6a and h), whereas anaphase stages displayed correct sister chromatid segregation (Figure 6b). Consequently, chromosomes were evenly divided between the poles in telophase midbody stages and cleavage furrow contraction is normally completed (Figures 6b, c and i).

In contrast, a significant proportion of siMITF cells exhibited mitotic defects (Figure 7), including several

DNA replication recombination and repair.

Gene	Fold change	MITF occupied	E-box
RPA	-3.2	NO	
FANCG	-2.3	NO	
RMI	-2.1	NO	
PIF1	-2.1	YES	
MCM5	-2.1	YES	~ -23 kB 5'-CACGTG-3'
POLM	-2.1	YES	~ -16 kB 5'-CATTTG-3'
LIG1	-2.1	YES	~ +5 kB 5'-CAGCTG-3' (Exon 2)
			~ +35 kB 5'-CAGCTC-3' (Intron 16)
RAD51L3	-2.0	YES	-39 5'-CAGATG-3'-33
CDT1	-2.0	YES	~ +8 kB 5'-CACGTG-3' (Downstream)
RECQL4	-2.0	NO	
MCM4	-1.9	NO	
PSMC3IP	-1.8	NO	
EME1	-1.8	YES	-256 5'-CACGTG-3' -251
CHTF18	-1.7	NO	
TERT	-1.6	YES	+30 5'-CACGTG-3' +25 (5'-UTR)
ORC6L	-1.6	YES	-454 54-CATGTG-3'-449
RFC5	-1.6	NO	
POLD1	-1.6	NO	
MCM2	-1.6	YES	+177 5'CACGTG-3' +182 (5'UTR)
FANCA	-1.6	YES	-2682 5'CACGTG-3' -2687
POLE2	-1.5	NO	
MCM6	-1.5	NO	
RAD54	-1.5	YES	~ -30 kB 5'-CATTTG-3'
CHAF1A	-1.5	YES	-64 5'-CAATTG-3'-59
XRCC3	-1.5	NO	
APEX2	-1.4	NO	
MDC1	-1.3	NO	
UIMC1	-1.3	NO	
BRCA1	-1.3	YES	+182 5'-CAGATG-3' +187 (Intron 1)
			~ +7 kB 5'-CACCTG-3' (Intron 2)
TDG	-1.3	YES	-22 5'-CACGTG-3' -17
MMS19	-1.3	YES	-90 5'-CACGTG-3'-95

Mitosis

Gene	Fold change	MITF occupied	E-box
ZNF114	-2.5	YES	-1486 5'-CAACTG-3' -1481
KIF4A	-2.2	NO	
ESPL1	-2.1	YES	~ -15 kB 5'-CAGGTG-3'
AURKB	-2.0	NO	
NUF2	-2.0	NO	
UPP1	-2.0	YES	~ -4 kB 5'-CAGCTG-3'
SPC25	-2.0	NO	
PLK1	-2.0	YES	-130 5'-CACGTG-3' -125
ALDH16A1	-1.9	NO	
KIFC1	-1.9	YES	-250 5'-CACGTC-3' -245
CDCA3	-1.8	NO	
CENPH	-1.7	YES	+254 5'-CAAGTG-3' +259 (Intron 1
ECT2	-1.7	NO	
PPP2CA	-1.6	NO	
C1ORF74	-1.6	NO	
NPM3	-1.6	NO	
CENPM	-1.6	YES	-127 5'-CACGTG-3' -132
			-13 5'-CACGTG-3' -18
CENPF	-1.6	YES	-193 5'-CACGTG-3'-188
CCNB1	-1.6	YES	-56 5'-CACGTG-3' -51
UBE2C	-1.6	NO	
SPC24	-1.5	YES	~ -11 kB 5'-CACGTG-3
MGAT4B	-1.5	NO	
NCAPD3	-1.5	NO	
TACC3	-1.5	YES	~ +28 kB 5'-CACGTG-3'
HAUS8	-1.5	YES	~ -4 kB 5'-CAGCTG-3'
DSN1	-1.5	NO	
CEP55	-1.5	NO	
HMBS	-1.5	NO	
GPRIN1	-1.5	YES	~ +4 kB 5'-CACATG-3' Exon1
SPAG5	-1.5	NO	
KIF20A	-1.4	NO	
CENPO	-1.4	NO	
SNW1	-1.4	NO	
TPX2	-1.4	NO	
CDCA8	-1.4	YES	-1723 5'-CATGTG-3' -1718
CCNF	-1.4	YES	No detected E box
NCAPD2	-1.4	NO	
CDC25B	-1.3	YES	+83 5'-CAGCTG-3' +88 (5'UTR)

Figure 4 MITF regulation of genes required for DNA replication, repair and mitosis. Genes involved in the above functions and identified as regulated by 3′-end RNA-seq following siMITF knockdown are listed along with the fold change in expression. For directly regulated genes, the location and sequence of the most prominent MITF-occupied E-box at each loci are indicated. Genes involved in each function were chosen based on the ontology and pathway analyses described in Figure 2. Additional genes involved in cell division were identified using the Mitocheck data base (http://www.mitocheck.org).

spindle and chromosome segregation defects, such as multipolar spindles with amplified centrosomes (Figure 6d), monopolar poles (data not shown), abnormal spindle structure with unfocused poles (Figures 6e–g), abnormal chromosome congression to the spindle equator and segregation failure (Figures 6e

and f), leading to uneven distribution of chromosomes in anaphase (Figure 6g). Three-dimensional reconstruction of confocal images of siMITF cells clearly showed chromosomes that did not align at the metaphase plate (arrows in Figure 6k). In addition, chromosome lagging was observed at telophase (Figure 6l). High magnifica-

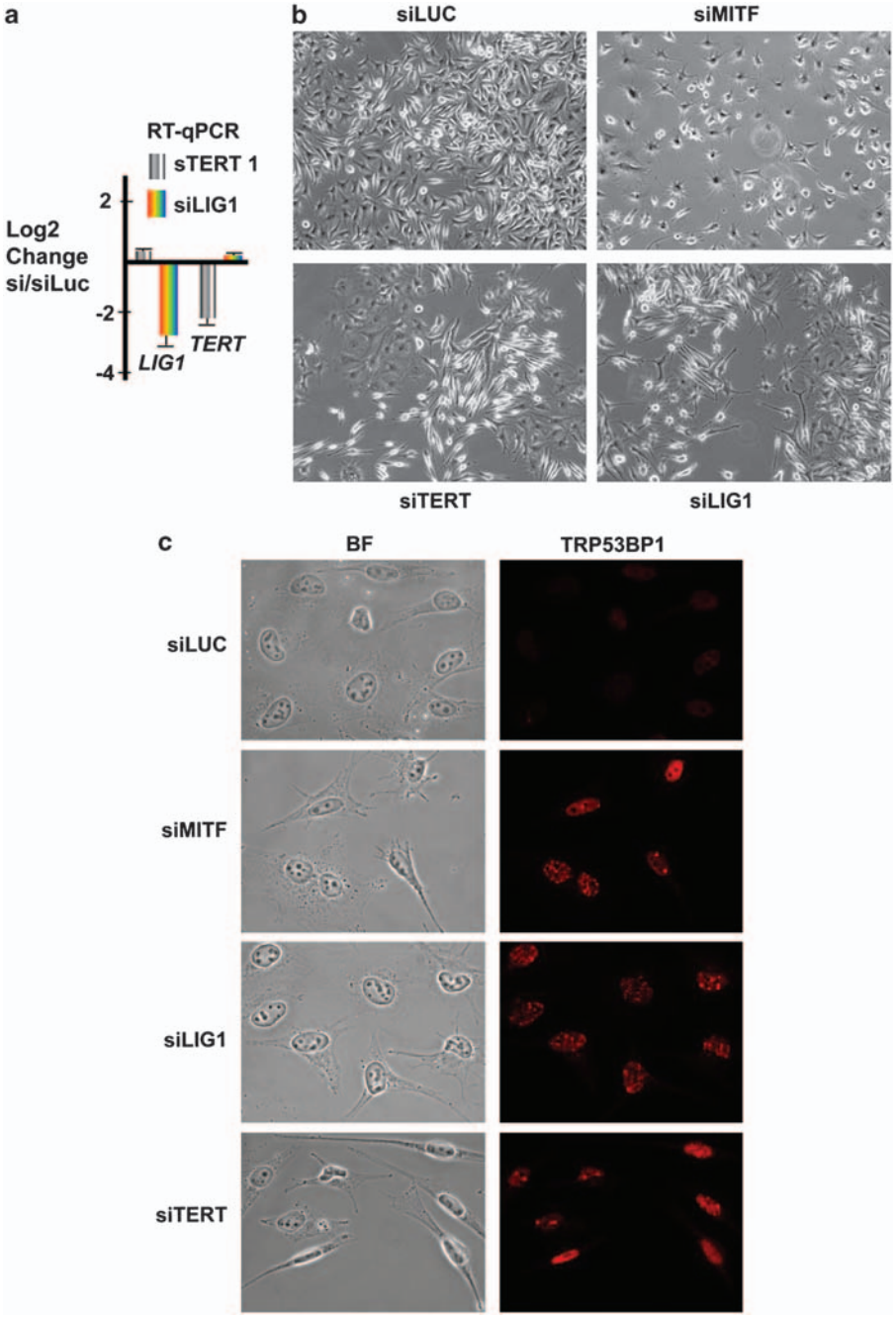

Figure 5 *LIG1* and *TERT* are required for normal 501Mel DNA replication. (**a**) Reverse transcriptase (RT)–qPCR of *LIG1* and *TERT* expression following the indicated siRNA-mediated knockdowns. (**b**) Phase contrast view of cells following siRNA-mediated knockdown. (**c**) Bright field (BF) view and staining with antibody against TRP53BP1 show that siMITF, siLIG and siTERT all lead to a potent activation of the DNA damage response.

Figure 6 Defective mitosis on MITF knockdown. (**a**–**c**) Labelling with β-tubulin (left panel), merged β-tubulin and phospho-serine 10 of H3 (centre panel) and Hoechst (right panel) of cells at 48 h after transfection with siLUC. (**d**–**g**) Analogous staining of cells transfected with siMITF. (**h**–**j**) Three-dimensional reconstruction of confocal microscopy images from siLUC-transfected cells. The insert in **j** shows a high-magnification view of the midbody. (**k**–**m**) Three-dimensional reconstruction of confocal microscopy images from siMITF-transfected cells. The insert in **l** shows lagging DNA that will not be incorporated into the daughter cell nuclei and the insert in **m** show a high-magnification view of the defective midbody. The arrows in **k** show chromosomes not aligned on the metaphase plate. (**n**–**o**) Labelling of siMITF-transfected cells with CENPA. The arrows indicate micronuclei with few or no centromeres.

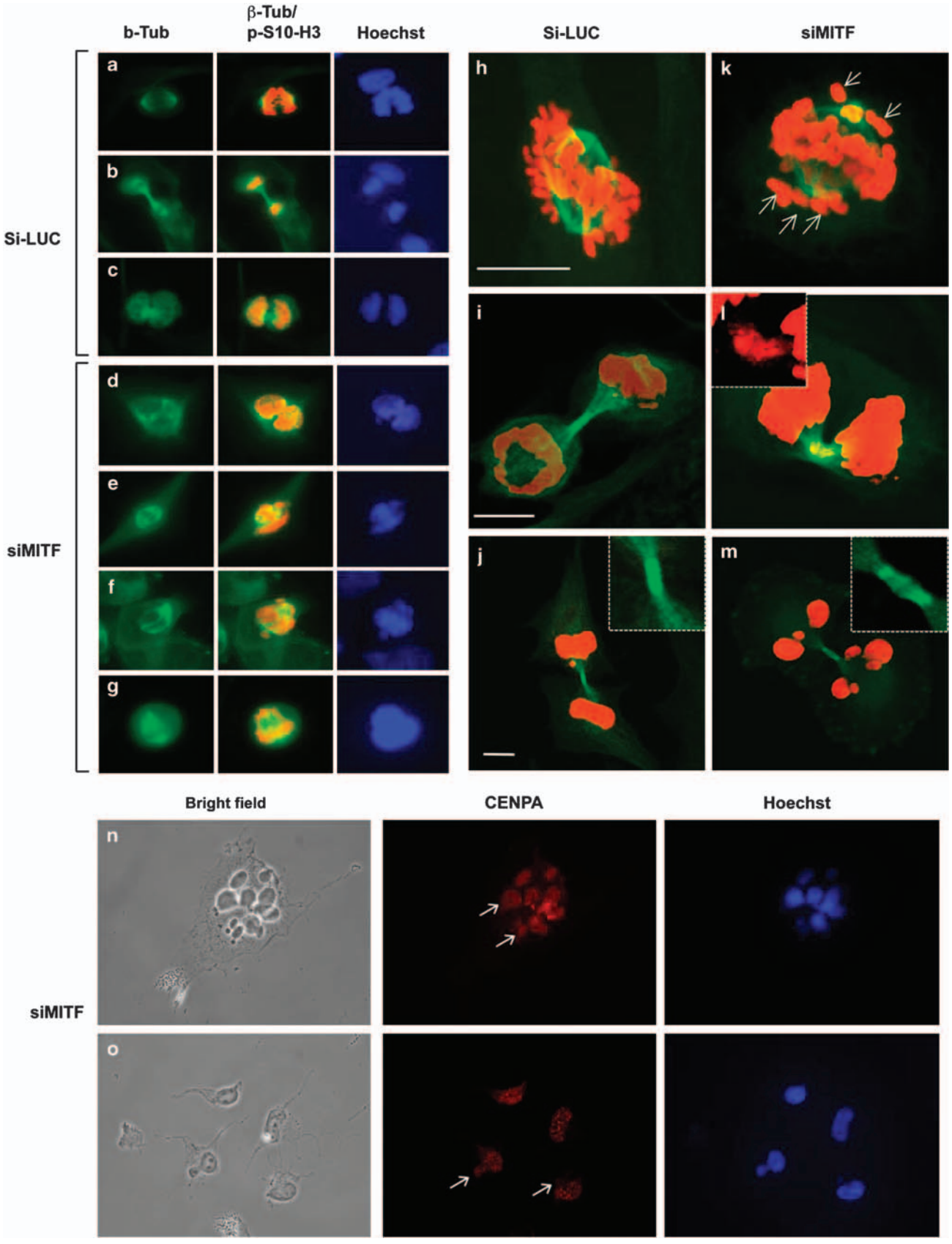
b-Tub
β-Tub/
p-S10-H3
Hoechst
Si-LUC
siMITF
a
b
c
d
e
f
g
h
i
j
k
l
m
Si-LUC
siMITF
Bright field
CENPA
Hoechst
n
o
siMITF

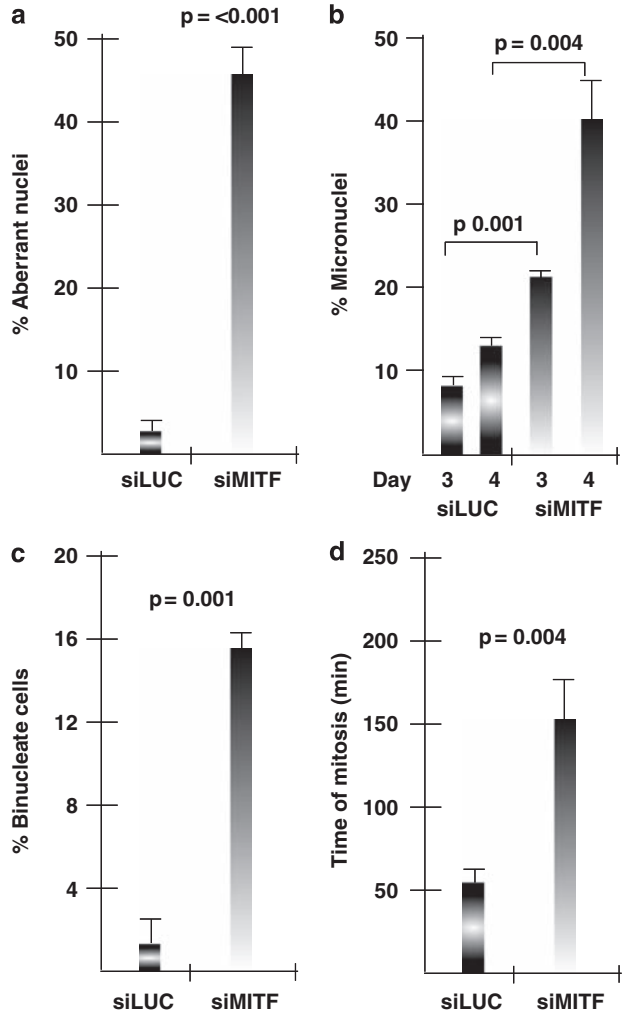

Figure 7 Mitosis defects in siMITF-knockdown cells. (**a**) Aberrant nuclei including polylobed nuclei, grape shaped nuclei and nuclei with anaphase bridges. (**b**) Micronuclei in siLUC and siMITF cells at 3 and at 4 days post transfection. (**c**) Binucleate cells were counted in siLuc and siMITF cells. (**d**) Control and MITF siRNA-transfected 501mel cells were video time-lapse recorded (Supplementary Movies 1 and 2) and the time (min) separating nuclear envelop breakdown from cytokinesis that corresponds to M phase was estimated in at least 10 cells.

tion showed the DNA that will likely be excluded from the reforming nuclei of the daughter cells and incorporated into micronuclei (Figure 7b).

Finally, we also observed significantly increased numbers of cell displaying persistent cytokinetic bridges and unresolved midbodies (Figure 6m, and data not shown). High-magnification views indicated that tubulin did not concentrate at the most apical midbody site between the dividing daughter cells compared with proper localisation observed in control cells (Figure 6j). Time-lapse video microscopy of melanoma cells transfected either with siLUC or siMITF, and synchronized in S phase with thymidine, revealed that the duration of mitosis was significantly longer in MITF-depleted cells than in siLUC consistent with the presence of mitotic defects (Figure 7d and Supplementary Movies 1 and 2).

As a result of chromosome lagging and mis-segregation, a significant increase in the percentage of cells with micronuclei that form during mitosis was observed (Figures 6n and o and Figure 7b). Many of these micronuclei did not contain centromeres (arrows in Figure 6n), consistent with chromosome fragmentation occurring with anaphase bridging. The appearance of acentric micronuclei has been associated with DNA damage, consistent with the observation that MITF depletion leads to defective replication and repair triggering activation of the DNA damage response (Giuliano *et al*., 2010 and Figure 5).

Discussion

Lineage-specific control of replication, mitosis and genome stability by MITF in melanoma

MITF is regarded as a lineage-specific oncogene that has a critical role in the pathogenesis of melanoma. Inhibition of MITF expression/activity has been shown to inhibit melanoma cell proliferation. However, it is not known whether this arrest is reversible, and the molecular mechanisms by which MITF controls cell proliferation and survival remained to be fully elucidated. Understanding the role of MITF in these processes will, therefore, help to clarify whether it is a potential target for therapeutic intervention in melanoma.

It has been proposed that MITF may regulate proliferation via control of cyclin-dependent kinase or cyclin-dependent kinase inhibitor expression (Du *et al*., 2004; Carreira *et al*., 2005). We confirm here that MITF regulates *CDKN1B* expression. Nevertheless, this does not fully account for the recent finding that MITF silencing causes a robust and irreversible melanoma cell cycle arrest associated with a DNA-damage dependent senescence phenotype (Giuliano *et al*., 2010), as *CDKN1B* is not a major factor in this senescence programme.

The DNA damage reported by Giuliano *et al*. was proposed to result from mitotic defects, but this required confirmation as no MITF-target genes involved in mitosis have been previously described. Our present results demonstrate that MITF regulates a set of genes required for normal DNA replication, repair and mitosis, showing how MITF bypasses senescence and promotes proliferation. Indeed, ChIP-seq and RNA-seq experiments reveal that MITF directly regulates several proteins involved in DNA replication (*LIG1*), genome maintenance (*TERT*, *EME1*, *BRCA1* and *FANCA*) and kinetochore function (*SPC24*, proteins of the CENP and chromosome passenger complex). Knockdown of these proteins may result in chromosome congression defects, kinetochore–microtubule attachment errors, lagging chromosome in anaphase and failure in cytokinesis consistent with the defects seen in siMITF-knockdown cells (Neumann *et al*., 2010). Moreover, downregulation of one component can lead to destabilisation and mislocalisation of other subunits, thereby

accentuating genome instability. These observations provide a molecular mechanism by which MITF directly regulates accurate chromosome segregation, in mitosis, and genomic stability and conversely how diminished MITF expression may lead to severe mitotic defects and senescence entry.

In other cell types, analogous DNA replication and mitotic defects often result in apoptosis. However, siMITF knockdown does not promote significant apoptosis, but instead entry into a senescence state that may be linked to the genetic background of melanoma cells, in which anti-apoptotic molecules, such as BCL2, are expressed, whereas the apoptosis effector APAF1 is repressed (Soengas and Lowe, 2003). The demonstration that an oncogenic transcription factor exerts its proliferative function by directly regulating a broad set of genes required for replication, repair and mitosis represents a unique mechanism of action.

The above observations explain the proliferative properties of MITF-expressing melanoma cells. It is also interesting to note that melanomas are notoriously resistant to chemo- and radiotherapies partly due to high expression of the DNA repair machinery. In line with this, MITF detection after chemotherapy treatment of patients with melanoma has been associated with a significantly lower relapse-free period and overall survival (Koyanagi *et al*., 2006). Elevated MITF expression in a sub-population of melanoma cells may confer this resistance through regulation of the repair machinery allowing them to reform tumours following treatment.

At the same time, cells transiently expressing low MITF level have been reported to exhibit low proliferative activity but enhanced motility and metastatic properties (Hoek *et al*., 2008a). In agreement with this, RNA-seq identifies MITF-regulated genes that are involved in adhesion, cell morphology motility and metastasis. In addition to *DIAPH1*-affecting cytoskeleton organisation that is downregulated, the expression of genes influencing metastasis, such as *MCAM* (Ouhtit *et al*., 2009), *SHC4* (also known as RaLP; Fagiani *et al*., 2007) and *BMP4* (Rothhammer *et al*., 2005), are upregulated. Interestingly, MITF occupies several sites upstream of the *SHC4* gene and a site in the first intron of the *MCAM* gene, and may, therefore, directly downregulate the expression of these genes.

The mechanisms that regulate MITF expression in tumours are not fully understood. However, the transforming growth factor β signalling pathway decreases MITF expression (Kim *et al*., 2004; Nishimura *et al*., 2010) and defines a population of cells with low proliferative, but high invasive properties (Hoek *et al*., 2006). We note that MITF knockdown upregulates expression of the transforming growth factor β3 ligand suggesting a positive feedback loop that maintains a low MITF pro-tumorigenic state. Furthermore, cells expressing high MITF show low POU3F2 expression and vice versa (Goodall *et al*., 2008; Pinner *et al*., 2009). This is in part explained by POU3F2 binding to the MITF-M promoter that represses its expression (Goodall *et al*., 2008; Kobi *et al*. 2010). However, siMITF also results in a strong increase in POU3F2 expression although there is no MITF-occupied site within 100 kb of the *POU3F2* locus (data not shown). There is, therefore, an intricate feedback loop of direct and indirect regulation between MITF and POU3F2 that controls their respective expression. Current models suggest that melanoma development involves the switching of the low-MITF expressing cells back to a proliferative state (Hoek *et al*., 2008a). Switching back to the proliferative state is a rare event (Pinner *et al*., 2009) in agreement with the idea that most of the low MITF cells show extensive DNA damage.

Together our observations allow us to extend the proposed 'rheostat' model for MITF function in melanoma (Carreira *et al*., 2006 and Figure 8). MITF

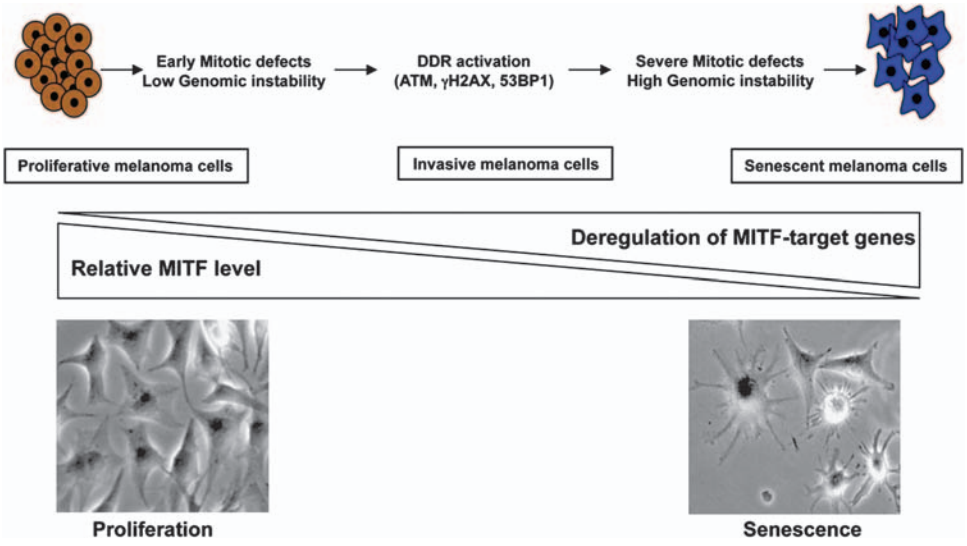

Figure 8 A rheostat model for MITF function. Schematic representation of the relationship between MITF expression and melanoma cell properties from proliferative cells (shown schematically, but also with image of normal proliferative 501Mel cells) with elevated MITF expression to invasive cells with lower levels and senescent cells (shown schematically, but also with image of siMITF 501Mel cells), in which MITF expression has been almost completely suppressed.

promotes proliferation through the activation of the genes encoding the DNA replication and repair machinery, and repression of genes that promote motility and invasion. Moreover, in cells expressing lower levels of MITF, proliferation is reduced and replicative and mitotic fidelity is diminished. The downregulation of replication and mitotic fidelity genes illustrates how lower levels of MITF may promote genomic instability favouring the transition to a more aggressive and invasive state. Under some circumstances, such as that obtained on siRNA silencing, the decrease in MITF levels below a specific threshold leads to severe replication and mitotic defects too severe to be repaired and cells enter in senescence. Therefore, acute MITF inhibition may be helpful in the treatment of melanoma. Our results do not, however, exclude the possibility that in melanoma tumours *in vivo*, decreased MITF expression could be offset by the upregulation of other pathways that suppress senescence and enable MITF-negative cells to develop and adopt an invasive profile. Similarly, normal melanocyte stem cells have little, if any MITF expression, but do not undergo senescence. It is possible, therefore, that only the combination of MITF depletion together with upregulation of mitogen-activated protein kinase signalling through, for example, activation of BRAF in melanoma, triggers senescence.

Our observations illustrate the concept of 'lineage addiction' (Garraway *et al*., 2005a), in which cellular functions that are normally controlled by diverse pathways are regulated in an integrated, coordinate and lineage-specific manner by a single transcription factor, in this case MITF. However, our results show how other oncogenic members of the basic helix-loop-helix family recognising E-box sequences, such as N-myc in neuroblastoma or TFE3 in alveolar soft part sarcoma and renal cell carcinomas may also function through regulation of similar sets of genes to control proliferation and genome stability.

Materials and methods

Transfection and culture of 501Mel cells expressing tagged MITF

Cells (501Mel) were cultured in RPMI 1640 medium (Sigma, St Louis, MO, USA) supplemented with 10% foetal calf serum. Cells were transfected with a porcine cytomegalovirus-based vector expressing 3× HA-tagged MITF and a vector encoding puromycin resistance. Transfected cells were selected with puromycin, and the expression of MITF verified by western blot using the antibody MITF: ab-1 (C5) from neomarkers or the 12CA5 HA antibody (Roche, Basel, Switzerland). Transient and stable transfections were performed with FuGENE 6 reagent (Roche) following the manufacturers instructions. The siRNA knockdown of MITF was performed with two independent and previously described sequences (Larribere *et al*., 2005; Carreira *et al*., 2006). Transfection was performed using Lipofectamine 2000 (Invitrogen, La Jolla, CA, USA).

ChIP-sequencing

ChIP and ChIP-seq experiments were performed on chromatin from native 501Mel cells or the clone 8 cells according to standard protocols as previously described (Delacroix *et al*., 2010; Kobi *et al*., 2010). Briefly, ChIP-seq was performed using an Illumina GAIIx sequencer (Illumina, San Diego, CA, USA) and the raw data analysed by the Illumina Eland pipeline V1.6 (Illumina). Peak detection was performed using the MACS software (http://liulab.dfci.harvard.edu/MACS/; Zhang *et al*., 2008) under settings, in which the HA–ChIP from untagged 501Mel cells was used as a negative control. Peaks were then annotated using GPAT (Krebs *et al*., 2008; http://bips.u-strasbg.fr/GPAT/Gpat_home.html) using a window of ±20 kb with respect to the coordinates of the beginning and the end of RefSeq transcripts. Further details are provided in the Supplementary Information.

RNA-sequencing

The 3′-end RNA sequencing was performed essentially as described in the digital gene expression protocol from Illumina. Duplicate RNA samples from siMITF or siLUC cells were prepared and a 3′-end tag from the polyA$^+$-containing fraction was isolated after generation of double-stranded complementary DNA and digestion with DpnII. Fragments were sequenced on the Illumina GAII platform and annotation was performed with the Ensembl tag table software (http://research.stowers-institute.org/microarray/tag_tables/index.html). Data sets were normalised using the Bioconductor DEseq package. (http://www.bioconductor.org/packages/2.6/bioc/html/DESeq.html).

Immunofluorescence and confocal laser scanning

Image acquisition and analysis were performed on the C3M MiCa Cell Imaging Facility (http://www.mica-bio.fr). Immunofluorescence on siMITF and siLUC cells was performed by standard procedures using the following antibodies: gH2AX (ab22551 Abcam, Cambridge, UK), HP1β (1A9), β-tubulin (2A2, Sigma, St Louis, MO, USA), histone H3 phospho-serine 10 (CS-116-100 Diagenode, Liège, Belgium), CENPA (no. 07-574 Upstate, Millipore, Billerica, MA, USA). Immunofluorescence was visualised with ×40 lens using a Zeiss Axiophot (Carl Zeiss, Göttingen, Germany) microscope equipped with epifluorescence illumination.

Confocal optical sections of cells were obtained with a Zeiss LSM510Meta microscope (Carl Zeiss) using a X63 NA1.4 plan-apochromat oil immersion lens. Excitation of 4′-6-diamidino-2-phenylindole, fluorescein isothiocyanate and Texas Red was performed with diode (405 nm), argon (488 nm) and HeNe (543 nm) lasers. The parameters of the system were adjusted to avoid saturation. Image stacks were saved and processed for three-dimensional reconstruction with Volocity 5 software (PerkinElmer, Waltham, MA, USA). Each stack consisted of a series of between 22 and 30 sections taken with a step size of 380 nm.

Time lapse

Cells were filmed for different periods of time, in constant conditions of 5% CO_2 at 37 °C, and observed by phase-contrast optics using an Axiovert 200 microscope (Carl Zeiss) with shutter-controlled illumination (Carl Zeiss) and a cooled, digital CCD camera (Photometrics CoolSNAP HQ, Roper Scientific, Trenton, NJ, USA) using a ×20 lens. Images were recorded at one frame per 20 min, and processed using NIH ImageJ version 1.43q analysis software (NIH, Bethesda, MD, USA) and QuickTime pro 5 software (Apple, Cupertino, CA, USA).

Further details of all experimental procedures are described in the Supplementary Information.

Conflict of interest

The authors declare no conflict of interest.

Acknowledgements

We thank B Jost for Illumina sequencing, A Hamiche and E Soutoglou for antibodies. This work was supported by grants from the CNRS, the INSERM, the Association pour la Recherche contre le Cancer grant 4985 and 7823, the Ligue Nationale contre le Cancer, the Institut national du Cancer grant R08009AP and the ANR Regulome project grant. We thank the Conseil Regional de la Région Provence-Alpes-Cote d'Azur, the Nice University Hospital and the Conseil Général des Alpes Maritimes for funding of the C3M MiCa Cell Imaging Facility. ID and CB are 'équipes labellisées' of the Ligue Nationale contre le Cancer.

References

Abraham J, Lemmers B, Hande MP, Moynahan ME, Chahwan C, Ciccia A *et al*. (2003). Eme1 is involved in DNA damage processing and maintenance of genomic stability in mammalian cells. *EMBO J* **22**: 6137–6147.

Artandi SE, DePinho RA. (2000). Mice without telomerase: what can they teach us about human cancer? *Nat Med* **6**: 852–855.

Artandi SE, DePinho RA. (2010). Telomeres and telomerase in cancer. *Carcinogenesis* **31**: 9–18.

Bentley DJ, Harrison C, Ketchen AM, Redhead NJ, Samuel K, Waterfall M *et al*. (2002). DNA ligase I null mouse cells show normal DNA repair activity but altered DNA replication and reduced genome stability. *J Cell Sci* **115**: 1551–1561.

Bentley NJ, Eisen T, Goding CR. (1994). Melanocyte-specific expression of the human tyrosinase promoter: activation by the microphthalmia gene product and role of the initiator. *Mol Cell Biol* **14**: 7996–8006.

Bertolotto C, Busca R, Abbe P, Bille K, Aberdam E, Ortonne JP *et al*. (1998). Different cis-acting elements are involved in the regulation of TRP1 and TRP2 promoter activities by cyclic AMP: pivotal role of M boxes (GTCATGTGCT) and of microphthalmia. *Mol Cell Biol* **18**: 694–702.

Beuret L, Flori E, Denoyelle C, Bille K, Busca R, Picardo M *et al*. (2007). Up-regulation of MET expression by alpha-melanocyte-stimulating hormone and MITF allows hepatocyte growth factor to protect melanocytes and melanoma cells from apoptosis. *J Biol Chem* **282**: 14140–14147.

Busca R, Berra E, Gaggioli C, Khaled M, Bille K, Marchetti B *et al*. (2005). Hypoxia-inducible factor 1\{alpha\} is a new target of microphthalmia-associated transcription factor (MITF) in melanoma cells. *J Cell Biol* **170**: 49–59.

Carreira S, Goodall J, Aksan I, La Rocca SA, Galibert MD, Denat L *et al*. (2005). Mitf cooperates with Rb1 and activates p21Cip1 expression to regulate cell cycle progression. *Nature* **433**: 764–769.

Carreira S, Goodall J, Denat L, Rodriguez M, Nuciforo P, Hoek KS *et al*. (2006). Mitf regulation of Dia1 controls melanoma proliferation and invasiveness. *Genes Dev* **20**: 3426–3439.

Carroll CW, Silva MC, Godek KM, Jansen LE, Straight AF. (2009). Centromere assembly requires the direct recognition of CENP-A nucleosomes by CENP-N. *Nat Cell Biol* **11**: 896–902.

Cheeseman IM, Chappie JS, Wilson-Kubalek EM, Desai A. (2006). The conserved KMN network constitutes the core microtubule-binding site of the kinetochore. *Cell* **127**: 983–997.

Chiaverini C, Beuret L, Flori E, Busca R, Abbe P, Bille K *et al*. (2008). Microphthalmia-associated transcription factor regulates RAB27A gene expression and controls melanosome transport. *J Biol Chem* **283**: 12635–12642.

Delacroix L, Moutier E, Altobelli G, Legras S, Poch O, Choukrallah MA *et al*. (2010). Cell-specific interaction of retinoic acid receptors with target genes in mouse embryonic fibroblasts and embryonic stem cells. *Mol Cell Biol* **30**: 231–244.

Du J, Widlund HR, Horstmann MA, Ramaswamy S, Ross K, Huber WE *et al*. (2004). Critical role of CDK2 for melanoma growth linked to its melanocyte-specific transcriptional regulation by MITF. *Cancer Cell* **6**: 565–576.

Dynek JN, Chan SM, Liu J, Zha J, Fairbrother WJ, Vucic D. (2008). Microphthalmia-associated transcription factor is a critical transcriptional regulator of melanoma inhibitor of apoptosis in melanomas. *Cancer Res* **68**: 3124–3132.

Fagiani E, Giardina G, Luzi L, Cesaroni M, Quarto M, Capra M *et al*. (2007). RaLP, a new member of the Src homology and collagen family, regulates cell migration and tumor growth of metastatic melanomas. *Cancer Res* **67**: 3064–3073.

Foltz DR, Jansen LE, Black BE, Bailey AO, Yates III JR, Cleveland DW. (2006). The human CENP-A centromeric nucleosome-associated complex. *Nat Cell Biol* **8**: 458–469.

Garraway LA, Weir BA, Zhao X, Widlund H, Beroukhim R, Berger A *et al*. (2005a). 'Lineage addiction' in human cancer: lessons from integrated genomics. *Cold Spring Harb Symp Quant Biol* **70**: 25–34.

Garraway LA, Widlund HR, Rubin MA, Getz G, Berger AJ, Ramaswamy S *et al*. (2005b). Integrative genomic analyses identify MITF as a lineage survival oncogene amplified in malignant melanoma. *Nature* **436**: 117–122.

Giuliano S, Cheli Y, Ohanna M, Bonet C, Beuret L, Bille K *et al*. (2010). Microphthalmia-associated transcription factor controls the DNA damage response and a lineage-specific senescence program in melanomas. *Cancer Res* **70**: 3813–3822.

Goding CR. (2000a). Mitf from neural crest to melanoma: signal transduction and transcription in the melanocyte lineage. *Genes Dev* **14**: 1712–1728.

Goding CR. (2000b). Melanocyte development and malignant melanoma. *Forum (Genova)* **10**: 176–187.

Gomez-Baldo L, Schmidt S, Maxwell CA, Bonifaci N, Gabaldon T, Vidalain PO *et al*. (2010). TACC3-TSC2 maintains nuclear envelope structure and controls cell division. *Cell Cycle* **9**: 1143–1155.

Goodall J, Carreira S, Denat L, Kobi D, Davidson I, Nuciforo P *et al*. (2008). Brn-2 represses microphthalmia-associated transcription factor expression and marks a distinct subpopulation of microphthalmia-associated transcription factor-negative melanoma cells. *Cancer Res* **68**: 7788–7794.

Hoek KS, Eichhoff OM, Schlegel NC, Dobbeling U, Kobert N, Schaerer L *et al*. (2008a). *in vivo* switching of human melanoma cells between proliferative and invasive states. *Cancer Res* **68**: 650–656.

Hoek KS, Schlegel NC, Brafford P, Sucker A, Ugurel S, Kumar R *et al*. (2006). Metastatic potential of melanomas defined by specific gene expression profiles with no BRAF signature. *Pigment Cell Res* **19**: 290–302.

Hoek KS, Schlegel NC, Eichhoff OM, Widmer DS, Praetorius C, Einarsson SO *et al*. (2008b). Novel MITF targets identified using a two-step DNA microarray strategy. *Pigment Cell Melanoma Res* **21**: 665–676.

Hou L, Pavan WJ. (2008). Transcriptional and signaling regulation in neural crest stem cell-derived melanocyte development: do all roads lead to Mitf? *Cell Res* **18**: 1163–1176.

Kim DS, Park SH, Park KC. (2004). Transforming growth factor-beta1 decreases melanin synthesis via delayed extracellular signal-regulated kinase activation. *Int J Biochem Cell Biol* **36**: 1482–1491.

Kim NW, Piatyszek MA, Prowse KR, Harley CB, West MD, Ho PL *et al*. (1994). Specific association of human telomerase activity with immortal cells and cancer. *Science* **266**: 2011–2015.

Kobi D, Steunou AL, Dembele D, Legras S, Larue L, Nieto L *et al*. (2010). Genome-wide analysis of POU3F2/BRN2 promoter occupancy in human melanoma cells reveals Kitl as a novel regulated target gene. *Pigment Cell Melanoma Res* **23**: 404–418.

Koyanagi K, O'Day SJ, Gonzalez R, Lewis K, Robinson WA, Amatruda TT *et al*. (2006). Microphthalmia transcription factor as a molecular marker for circulating tumor cell detection in blood of melanoma patients. *Clin Cancer Res* **12**: 1137–1143.

Krebs A, Frontini M, Tora L. (2008). GPAT: retrieval of genomic annotation from large genomic position datasets. *BMC Bioinformatics* **9**: 533.

Larribere L, Hilmi C, Khaled M, Gaggioli C, Bille K, Auberger P *et al*. (2005). The cleavage of microphthalmia-associated transcription factor, MITF, by caspases plays an essential role in melanocyte and melanoma cell apoptosis. *Genes Dev* **19**: 1980–1985.

Levy C, Khaled M, Robinson KC, Veguilla RA, Chen PH, Yokoyama S *et al*. (2010). Lineage -specific transcriptional regulation of DICER by MITF in melanocytes. *Cell* **141**: 994–1005.

McGill GG, Horstmann M, Widlund HR, Du J, Motyckova G, Nishimura EK *et al*. (2002). Bcl2 regulation by the melanocyte master regulator Mitf modulates lineage survival and melanoma cell viability. *Cell* **109**: 707–718.

Moore R, Champeval D, Denat L, Tan SS, Faure F, Julien-Grille S *et al*. (2004). Involvement of cadherins 7 and 20 in mouse embryogenesis and melanocyte transformation. *Oncogene* **23**: 6726–6735.

Neumann B, Walter T, Heriche JK, Bulkescher J, Erfle H, Conrad C *et al*. (2010). Phenotypic profiling of the human genome by time-lapse microscopy reveals cell division genes. *Nature* **464**: 721–727.

Nishimura EK, Suzuki M, Igras V, Du J, Lonning S, Miyachi Y *et al*. (2010). Key roles for transforming growth factor beta in melanocyte stem cell maintenance. *Cell Stem Cell* **6**: 130–140.

Ouhtit A, Gaur RL, Abd Elmageed ZY, Fernando A, Thouta R, Trappey AK *et al*. (2009). Towards understanding the mode of action of the multifaceted cell adhesion receptor CD146. *Biochim Biophys Acta* **1795**: 130–136.

Pinner S, Jordan P, Sharrock K, Bazley L, Collinson L, Marais R *et al*. (2009). Intravital imaging reveals transient changes in pigment production and Brn2 expression during metastatic melanoma dissemination. *Cancer Res* **69**: 7969–7977.

Rothhammer T, Poser I, Soncin F, Bataille F, Moser M, Bosserhoff AK. (2005). Bone morphogenic proteins are overexpressed in malignant melanoma and promote cell invasion and migration. *Cancer Res* **65**: 448–456.

Ruchaud S, Carmena M, Earnshaw WC. (2007). Chromosomal passengers: conducting cell division. *Nat Rev Mol Cell Biol* **8**: 798–812.

Rudolph KL, Chang S, Lee HW, Blasco M, Gottlieb GJ, Greider C *et al*. (1999). Longevity, stress response, and cancer in aging telomerase-deficient mice. *Cell* **96**: 701–712.

Schmit TL, Zhong W, Setaluri V, Spiegelman VS, Ahmad N. (2009). Targeted depletion of Polo-like kinase (Plk) 1 through lentiviral shRNA or a small-molecule inhibitor causes mitotic catastrophe and induction of apoptosis in human melanoma cells. *J Invest Dermatol* **129**: 2843–2853.

Soengas MS, Lowe SW. (2003). Apoptosis and melanoma chemoresistance. *Oncogene* **22**: 3138–3151.

Steingrimsson E. (2008). All for one, one for all: alternative promoters and Mitf. *Pigment Cell Melanoma Res* **21**: 412–414.

Tomkinson AE, Mackey ZB. (1998). Structure and function of mammalian DNA ligases. *Mutat Res* **407**: 1–9.

Wang W. (2007). Emergence of a DNA-damage response network consisting of Fanconi anaemia and BRCA proteins. *Nat Rev Genet* **8**: 735–748.

Wu G, Lin YT, Wei R, Chen Y, Shan Z, Lee WH. (2008). Hice1, a novel microtubule-associated protein required for maintenance of spindle integrity and chromosomal stability in human cells. *Mol Cell Biol* **28**: 3652–3662.

Zhang Y, Liu T, Meyer CA, Eeckhoute J, Johnson DS, Bernstein BE *et al*. (2008). Model-based analysis of ChIP-Seq (MACS). *Genome Biol* **9**: R137.

Supplementary Information accompanies the paper on the Oncogene website (http://www.nature.com/onc)